SLAC-PUB-1134
(ACC)
October 1972

CURRENT STATUS OF SUPERCONDUCTING ACCELERATOR TECHNOLOGY*

P. B. Wilson
Stanford Linear Accelerator Center
Stanford University, Stanford, California 94305

Superconducting accelerator technology is celebrating an anniversary this year. Ten years ago, in 1962, Q's in the range 10^8-10^9 and peak rf mangetic fields on the order of 100 G were obtained in measurements on lead-plated, S-band cavities at Stanford. While the theoretical possibility of building superconducting linear accelerators had been considered previously, these results marked, if not the birth, then at least an important turning point in the history of this new technology. In the years immediately following, further improvements in rf cavity properties and advances in cryogenic technology, due in large part to the efforts of the Stanford group, continued to point the way toward the practical realization of superconducting accelerators. Plans were made at Stanford and at other laboratories around the world for the construction of a superconducting accelerator or an rf separator. At present, something like 15 laboratories have under construction, or are seriously proposing, devices using superconducting rf structures. After a decade of escalating effort directed toward superconducting accelerator development, the time seems appropriate for a survey of the activity in this field.

A summary† in any real depth of the current status of superconducting accelerator technology poses a formidable task, and perhaps the title of this paper promises too much. Let us consider instead the following, more specific, questions: What is happening at the present time in the field of superconducting accelerator (SCA) research, development and construction? What are the limitations currently being encountered in superconducting cavities and structures? Are these limitations understood, and how might they be overcome? The first of these questions is relatively straightforward, and in the next section an answer has been attempted in the form of a summary of the activities of the various laboratories around the world involved in SCA projects. In the remainder of the paper we address ourselves to the second and third questions by picking out two specific limitations on superconducting cavities for consideration, using some experimental and theoretical results obtained at SLAC.

Current SCA Activity

In Tables I and II, some of the long range goals, immediate objectives, problems currently under investigation, and recent experimental results are listed for a number of laboratories in the United States and overseas which are working on SCA projects. At one laboratory the emphasis is primarily on superconducting electron linac development; three laboratories are developing superconducting rf separators for use with proton synchrotrons; four institutes are considering cyclic electron accelerators (synchrotrons, microtrons, mesotrons) using superconducting rf systems; six laboratories are engaged in the development of superconducting proton or heavy-ion accelerators. Several laboratories are working on more than one project, and several more consider their program as applied research on rf superconductivity, with applications in other areas besides accelerator technology.

The listing presented here does not pretend to be complete. For example, the work[22] on electropolishing and anodizing carried out at Siemens Research Laboratories (Erlangen, West Germany) has made a very direct contribution to SCA technology. Some smaller projects, or projects that have only recently been initiated may have been overlooked. It recently came to the author's attention that electrons have been accelerated at Osaka University, Japan, using a superconducting cylindrical cavity. Also in Japan, the National Laboratory for High Energy Physics has recently started a program of research on superconducting cavities and SCA development, [30] and at Tohoku University there is interest in such a project. Finally, answers to inquiries sent to the USSR have not been received in time for inclusion here. In the past, however, there has been work on superconducting cavities and structures at both the Physico-Technical Institute and the Physico-Technical Institute for Low Temperatures, in Kharkov.[23, 32] Superconducting resonators employing Nb-Ti surfaces have been studied at JINR, Dubna, with application in mind to an accelerating structure for a collective field (electron ring) accelerator.[31]

As the entry for SLAC in Table I implies, there is currently no funding for work on rf superconductivity at SLAC, and no activity is planned for the immediate future. An entry for SLAC has been included anyway because the project has been active until recently, and may again become active in the future should funding become available.

Even a casual glance at the two tables will indicate that several large SCA projects are now well underway. Stanford, in particular, has set ambitious goals and has already met most of them: for accelerated beam current, for energy stability and resolution, for large scale refrigeration and cryogenic component development, and for superconducting accelerator instrumentation and control. Only in the case of the energy gradient have experimentally measured values fallen below initial design expectations. The record of solid achievement made to date in the field of SCA technology is impressive, giving every promise that operational machines will soon be realized. But it is also clear that, if the potential of rf superconductivity in high field devices such as accelerators and rf separators is to be fully exploited, a better understanding of the limitations on the fields that can be attained in superconducting cavities is needed. One aspect of this problem is considered in the next section.

Effect of Exposure to Gases

It has been observed on numerous occasions that the Q and the peak obtainable field for a superconducting cavity often degrade in a poor vacuum system. Reproducible results from run to run are usually only obtained for "pinched-off" cavities; that is, cavities having a low temperature rf window separating the cavity vacuum from the room temperature vacuum system. Even more marked, exposure to air causes serious degradation for cavities initially having very high Q's and breakdown fields as the result of high temperature processing. Apparently, a clean niobium surface acts as a good "getter," with a strong affinity for one or more of the component gases normally found in air. A series of exposures to various

* Work supported by the U. S. Atomic Energy Commission.

(Presented at the Conference on Proton Linear Accelerators, Los Alamos, New Mexico, October 10-13, 1972.)

TABLE I

SUPERCONDUCTING ACCELERATOR PROJECTS IN THE UNITED STATES

Laboratory*	Long Range Goals; General Objectives	Immediate Objectives; Prototype Accelerators or Structures	Problems of Current Interest	Recent Results
Argonne National Laboratory	Heavy-ion accelerator: 20 MeV (terminal voltage) tandem electrostatic accelerator followed by 50 m long superconducting linac. Final energy 10 MeV per nucleon.	Construction of a prototype accelerator consisting of two superconducting helix rf cavities (f= 63 MHz, axial field = 2 MV/m) with associated electronic circuitry for phasing and for locking to a master oscillator. Protons will be injected at 0.8 MeV from a Van de Graaff.	Optimization of processing techniques for anodically oxidized niobium helices. Radiation damage. Methods for phasing successive resonators in the presence of mechanical vibrations.	An anodized niobium helix was exposed to air for 90 days, followed by a high field test run for 323 h at E(axial) = 2.5 MV/m. $Q_0 = 3 \times 10^8$ at E(axial) = 2.0 MV/m.[1],[28]
Brookhaven National Laboratory	Basic investigation of materials for superconducting rf cavities and structures, with emphasis on potential application to superconducting rf separators for high energy proton synchrotrons.	Construction of a 10 cell π-mode X band structure as a prototype for an rf separator at NAL.	Effect on Q_0 and peak fields of processing at high temperature in the presence of various gases. Investigation of alternative type II superconducting surfaces (e.g., Nb_3Sn, Nb-1% Zr). Investigation of surface effects on the superconducting properties of niobium.[3]	$Q_0 = 2 \times 10^9$, $H_p = 360$ G reached in 5 cell, $\pi/2$-mode S-band deflecting structure. $Q_0 \approx 1 \times 10^9$, $H_p = 250$ G attained for S-band cavity with Nb_3Sn surface.[2] Significant degradation in both Q_0 and H_p was produced in an anodized cavity by irradiation with $\sim 10^{15}$ protons/cm^2.[4]
California Institute of Technology	Heavy ion accelerator.	Assembly of several independent $\lambda/2$, 40 MHz lead-plated helix resonators, using a "building block" approach, to form a prototype structure.	Electric field loading in lead-plated helical resonators. Investigation of alternative structures (e.g., spiral structure) with high shunt impedance at low phase velocities.	Control circuitry developed for locking phase of field in a helical resonator to an external reference oscillator. Resonator frequency controlled by external variable reactance[5] Low-loss sapphire support structure tested at high field levels.[5] Accelerating field of 1.3 MV/m, and peak surface field exceeding 700 G, achieved in lead-plated helix resonator.
Cornell University	25-40 GeV electron synchrotron with a superconducting rf system.	Prototype structure (11 cell, 2856 MHz) to be installed and tested in the existing Cornell electron synchrotron. The design gradient is 3-6 MeV/m, preferably to be obtained without high temperature processing.	Design of a nonintercepting (in the horizontal plane) stub-loaded structure suitable for use in regions of high synchrotron radiation. Initial development of facilities for producing, processing and testing superconducting cavities and structures.	A Q_0 of 3×10^8 and E_{acc}=1-1/2 MeV/ft obtained for an anodized, single-cell S-band cavity. Carbon detected at grain boundaries on niobium surfaces using electron microscope and electron microprobe.
University of Illinois	600 MeV microtron with 1.3 GHz superconducting rf accelerating structure. Structure length 4.6 m; energy gain per pass, 30 MeV; output current 10 μA at 100% duty factor.[6]	Recirculation of beam for 3 to 6 turns using temporary bending magnets. Final beam energy 18-36 MeV for a design gradient of 1.0 MeV/ft.	Methods for increasing the gradient and Q of the niobium linac structure. Optimization of beam recirculation on the first several turns.	Electrons accelerated to 1.0 MeV (gradient $\approx$ 0.8 MeV/ft) by injector section.[7] Beam accelerated to 3.6 MeV (gradient $\approx$ 0.6 MeV/ft) in a 7-1/2 ft structure which had not been high-temperature processed.

*Unreferenced data and information were supplied by: ANL. R. Benaroya; BNL, H. Halama and H. Hahn; CIT, G. J. Dick; Cornell, M. Tigner and R. Sundelin; Illinois, A. O. Hanson; ORNL, C. M. Jones; Stanford-A, H. A. Schwettman; Stanford-B, I. Ben-Zvi

Table I (cont.)

Laboratory	Long Range Goals; General Objectives	Immediate Objectives; Prototype Accelerators or Structures	Problems of Current Interest	Recent Results
Oak Ridge National Laboratory	Heavy ion accelerator.	Continuation of tests on lead-plated helical resonators at 136 MHz.	Development of circuitry for phase locking to an external oscillator using an external variable reactance to control resonator frequency.	An axial accelerating field of 0.7 MV/m was obtained in a lead-plated helical resonator at 136 MHz.[8]
Stanford University (High Energy Physics Laboratory) A.	Development and exploitation of superconducting electron linacs for intermediate and high energy physics.[9] Basic investigation of rf superconductivity.	Construction of 1 sector (80 ft plus injector) during 1973; running operational tests of significant duration. Operational goals: energy, 75 MeV; current, > 100 μA; energy resolution, < 15 keV; duty cycle, 100%; beam emittance, $\Delta r \cdot \Delta\theta = 0.1$ mm-mrad; phase spread, 1.2°. Construction of a beam transport system for recirculating the beam up to 4 times through the rf structure (final energy ~275 MeV).	Investigation of methods for recirculation.[10] Investigation of electron loading effects in superconducting cavities and structures. Development of a 50 micron free electron laser. Design and contruction of a 3 m accelerating structure at 2600 MHz. Continued development of superconducting cavity stabilized oscillators; 10^{-14} stability recently achieved.[29]	A beam current of 290 μA was accelerated to 8 MeV in the linac injector (E_{acc} = 1.1 MV/ft).[11] A peak rf magnetic field of 350 G was reached in a TM test cavity at 1300 MHz.[12] A gradient of 2 MeV/ft (350 G peak magnetic field) was reached in a 7 cell structure at 2856 MHz.[12] A peak magnetic field of 650 G was attained in a TM mode S-band cavity.[12] Measurements of beam breakup have been made.[27] Methods have been devised for increasing the threshold current.
Stanford University B.	Development of superconducting structures and associated electronic control circuitry for heavy ion accelerators.	Construction of two re-entrant cavities at 433 MHz with electronic control circuitry; installation on a Van de Graaff injector.	Development of a piezoelectric tuner and control circuitry for locking to an external oscillator. Study of beam dynamics and alternating gradient focussing. Operation of a two-cavity prototype.	Unloaded Q's greater than 10^9 and peak surface electric field up to 26 MV/m were achieved in a re-entrant niobium cavity at 350 MHz.[13] A theory has been developed and verified experimentally for ponderomotive oscillations in helical resonators.[14]
Stanford Linear Accelerator Center	Investigation of rf superconductivity directed toward reaching high Q's and fields in cavities and prototype structure.	No activity planned for the immediate future. See text.	Investigation of alternative type II superconductors for rf applications, in particular niobium nitride. Investigation of the role of carbon in residual loss and magnetic field breakdown.	Magnetic breakdown fields > 1000 G and residual Q's > 10^{10} obtained in several TM mode cavities at 8.6 GHz. Effect of exposure to various gases measured. See Table III.

TABLE II

SUPERCONDUCTING ACCELERATOR PROJECTS OUTSIDE THE UNITED STATES

Laboratory*	Long Range Goals; General Objectives	Immediate Objectives; Prototype Accelerators or Structures	Problems of Current Interest	Recent Results
Karlsruhe (Institut für Experimentelle Kernphysik)	500-1000 MeV superconducting proton linac with 1 mA beam current at 100% duty cycle.	Completion of 20 m of anodized helix structure at 90 MHz to accelerate protons to 20 MeV. Construction of a pilot accelerator with a final energy in the region of 50 MeV and a current of 1 mA.[15]	Optimization of fabrication and processing techniques for anodized helices. Development of an rf feedback system to phase-lock separate helix arrays to master oscillator.[19] Design of an iris loaded structure at 720 MHz. Continuing theoretical and experimental work on problems of magnetic field breakdown, electron loading and residual loss.	In a coupled array of 5 helices, an axial accelerating field of 1.4 MV/m was obtained with peak surface fields of 530 G and 18 MV/m and an improvement factor of 2×10^4.[16] A 1.3 μA proton beam was accelerated at a gradient of 1.3 MV/m.[15]
Karlsruhe-CERN	Two 2.8 m long superconducting rf separator cavities for installation at CERN. Frequency, 2855 MHz; deflecting field gradient; 2 MV/m; peak surface fields, 310 G and 11 MV/m.[17]	Production of two test deflectors of 4 cells each to test final fabrication and processing techniques. Tests on a 22 cell module.	Optimization of fabrication and processing techniques for deflecting structures.	Magnetic breakdown fields in the range 250-510 G and Q's (at H_D) in the range $0.2\text{-}1.4 \times 10^9$ obtained in measurements on 4, 8 and 12 cell test deflectors. See also Ref. 17.
Orsay (Institut d'Electronique Fondamentale)	Basic studies of rf superconductivity with potential applications to electron linacs and electronic devices (stable oscillators, etc.).	Study single-cell TM-mode S-band cavities.	Optimization of processing techniques using recently acquired high temperature furnace.	Unloaded Q's $\sim 10^9$ obtained at S-band without high temperature processing.
Rutherford High Energy Laboratory	Two lead-plated, 1.2 m long (10 cells, π-mode, 1.3 GHz) separator cavities for installation at Nimrod. Design deflecting gradient, 2.5 MV/m; peak surface fields, 375 G and 9.3 MV/m.[18]	Completion of operational prototype separator by December 1972.	Development of new plating system using a "closed circuit" principle rather than open baths.	Peak surface fields of 410 G and 9.9 MV/m reached at $Q_0 \approx 2 \times 10^8$ in 3-cell lead-plated test structure.[18]
DESY	Construction initially of a microtron with the possibility of the eventual construction of a high energy (30-60 GeV) "mesotron"[20] type of electron accelerator.	Solid niobium cavity operating at L-band under construction.		
Bonn (Technical Institute, University of Bonn)	Mesotron[20] type of accelerator.	Tests to begin on short model cavities at X-band.		
Weizmann Institute of Science (Israel)	Heavy-ion accelerator: 14 MeV (terminal voltage) tandem electrostatic accelerator coupled with a 20 MeV booster linac using separately phased re-entrant superconducting cavities.	Superconducting cavity development for eventual application to this project is at present proceeding at Stanford University (see Table I, Stanford University B).		

*Unreferenced data and information were supplied by: Karlsruhe, M. Kuntze; Karlsruhe-CERN, H. Lengeler; Orsay, V. Nguyen; RHEL, A. Carne; DESY, E. Freytag; Weizmann Institute, I. Ben-Zvi.

pure gases were made at SLAC in an attempt to find which of the gases usually present in air or in a poor vacuum system might produce damaging effects.

Some preliminary results†† for several series of exposures are given in Table III. The exposures were

TABLE III: SUMMARY OF GAS EXPOSURE TESTS

Gas	Residual Q Before	Residual Q After	Breakdown Field Before	Breakdown Field After	Q Jumping Factor
Series 1					
H_2	7×10^9	6×10^9	640 G	696 G	1^+
Dry O_2	6×10^9	4×10^9	696	660	1
Wet O_2 (trace CO_2)	4×10^9	1.6×10^9	660	361	3
Air	1.6×10^9	3×10^8	361	343	3
Series 2					
CO_2	$>5\times10^{10}$	1×10^9	1073	208	2-1/2
Series 3					
CO	7×10^9	8×10^9	1042	684	20
CO_2	8×10^9	1×10^9	684	331	2-1/2
Series 4					
CH_4	6×10^9	1.3×10^9	1000	390	1^-
O_3	1.3×10^9	7×10^8	390	255	2-1/2

made at room temperature for a period of about one hour at a pressure on the order of 1/4 atmosphere. In the table the residual Q before and after exposure is listed, along with the breakdown field before and after exposure and a parameter called the Q jumping factor. This factor is the ratio of the Q at low power (usually measured at about 1.5° K) after the application of high rf power, to the low power Q before the initial application of high power. It is a measure of the processing that the cavity has undergone. Note that carbon dioxide produces the most damaging effects, while methane (found as a residual gas in systems pumped with ion pumps) is almost as deleterious. Carbon monoxide is considerably less damaging, while hydrogen and dry oxygen are benign. All of the cavities are initially assembled in nitrogen, and so this gas can also be ruled safe (at least if there are no contaminants present, a situation which is not always easy to achieve). The effect of a gas exposure is most noticeable for cavities which are initially very good. Even after a carbon dioxide exposure, the residual Q tends to end up at 1×10^9, while the breakdown field is lowered to the 200-300 G range. For a poor cavity which already has a Q and breakdown field of this order, no effect would be observed on exposure to CO_2, while in the case of a really good cavity the degradation would not be tolerable.

Physically, what is happening to cause such severe effects, when it might be expected that only a molecular layer or so of gas will be absorbed on the niobium surface? Why does the applications of rf power cause a permanent increase in Q? One can postulate a migration of the absorbed gas laterally over the niobium surface from one pinning site to the next, driven by the interaction of the electric or magnetic dipole moment of the gas with the rf field. However, to the author's knowledge, no really satisfactory model has as yet been developed which fully explains the experimental observations.

What are the implications of these measurements for superconducting accelerators? It seems clear that, to maintain the highest Q's and breakdown fields, either the surfaces of cavities that have been high temperature fired must not be exposed to air or to the contaminants in a poor vacuum system, or else the surface must be protected by anodizing (which can in itself degrade the Q for modes with a surface electric field) or by the deposition or formation of some other type of protective layer. Taking the latter approach at SLAC, we have been working toward the development of niobium nitride as an alternative, more stable superconducting surface. We have been able to get a good NbN layer††† with a high (~ 17°K), narrow (~ .01°K) transition on niobium test strips, but have not yet managed to put such a surface on a cavity. At Brookhaven, niobium-tin is being investigated, and some initial results appear promising (see Table I).

Limitations on Peak RF Fields

The maximum field attainable in a superconducting cavity or structure is typically limited by one of several effects. Electric field loading effects, such as field emission or multipactor, may occur. Other related regenerative effects involving electron transits across the cavity, but which are not yet well understood, may also take place. Electric field loading is relatively worse at lower frequencies, and for L-band cavities often sets the limit on the attainable field.[12] The rf magnetic field may be limited in at least two ways. If the unloaded Q is low, or if the thermal impedance between some portion of the cavity surface and the liquid helium bath is too high, then at some field level a situation may be reached such that a further increase in incident power results in a rapid increase in loss, a consequent decrease in Q, and no appreciable increase in field. Particularly if the cavity is undercoupled, macroscopic heating of this type may result in a well defined (but stable) upper limit on the field.

What we will call here magnetic field breakdown (sometimes called "magnetic-thermal breakdown")[26] results from a different, highly localized type of heating. Presumeably, microscopic imperfections on the superconducting surface act as centers of enhanced loss. At some field level a thermal run-away situation occurs in which the area surrounding the defect suddenly goes normal. The Q drops by several orders of magnitude and the stored energy in the cavity is nearly completely dumped, all this happening in a microsecond or so. The effect is completely reversible, and after the breakdown occurs the the cavity immediately begins to fill back toward its former field level having suffered no permanent degradation.

Many types of defects could produce the localized heating which in turn leads to magnetic field breakdown: geometric imperfections, such as steps and whiskers, which can enhance the local magnetic field; small regions of impurities, such as carbon clumps at a grain boundary; a region of lossy dielectric on the surface; dust particles on the surface. It has often been postulated that, as the area of a cavity is increased, the chances are also increased for finding ever worse defects somewhere on the surface. Since breakdown of this type is controlled by the worst defect present anywhere on the surface (assuming for simplicity a uniform rf field over the surface), a larger area implies a lower breakdown field. Turneaure[21] has shown that in measurements made on a wide variety of cavities, the maximum attainable breakdown field is a monotonically decreasing function of cavity area. In the following section we will put this intuitively reasonable model for the frequency dependence of magnetic field breakdown on an analytical basis.

Statistical Model for Magnetic Field Breakdown

Assume that, in the absence of any defect, the magnetic breakdown field for a perfectly homogeneous surface is H_{b1}. This field may be less than the critical field for the pure bulk material because the surface layer may contain a uniform impurity concentration which is considerably higher than that present in the bulk. Next, let us characterize an imperfection or defect by a reduction factor r, such that rH_{b1} would give the breakdown field if there were only this single defect on the surface. We intuitively expect that on a real surface there will be a very large number of defects with r just a little less than unity, while there will be a vanishingly small number of defects having values of r approaching zero. A reasonable form for the distribution function giving the relative number of defects present on a surface, as a function of the reduction factor r, is shown in Fig. 1. Here $n'(r)dr$ gives the average number of defects per unit area in the range between r and (r + dr). The average number of defects per unit area having a reduction factor equal to or less than r is $n(r) = \int_0^r n'(r)dr$. A particular processing technique is characterized by the function n(r). Assuming that defects occur on a surface in a statistically random way and follow a Poisson distribution, the probability that there are no defects on a surface of area A with an enhancement factor equal to or less than r is

$$P_0[An(r)] = \exp[-An(r)] = \{p_0[n(r)]\}^A$$

This is also the probability that a cavity will not break down at $H_b < rH_{b1}$, or that it will break down at $H_b > rH_{b1}$. If we were to build a large ensemble of N_0 cavities, all fabricated by, as best we can tell, the same method (the statistical variation is due to all those factors which are not under our control), then the distribution function for the relative number of cavities breaking down as a function of r is

$$\frac{N(r)}{N_0} = -\frac{dp_0(r)}{dr} = A\frac{dn(r)}{dr}e^{-An(r)} \qquad (1)$$

where N(r)dr gives the number of cavities with breakdown fields in the range between rH_{b1} and $(r + dr)H_{b1}$. Thus, the function n(r) uniquely determines the distribution function N(r) for any cavity area (and hence frequency). Likewise, if N(r) is specified for any area (frequency), the breakdown field distribution function for any other area (frequency) is determined, assuming an identical processing technique.

To make these ideas more concrete, let us assume a physically reasonable and mathematically convenient functional form for n(r):

$$n(r) = \left[\frac{1 - r_1}{r_1}\right]^\alpha \left[\frac{r}{1-r}\right]^\alpha, \quad n(r_1) = 1 \qquad (2)$$

Plots of n(r) for several values of r_1 and α are given in Fig. 2. The value of α determines the sharpness of the "knee" in the curve, and also how fast n(r) approaches zero or infinity as r approaches zero or unity. Substituting Eq. (2) in Eq. (1), the corresponding distribution functions for the relative number of cavities breaking down as a function of field level are readily calculated. Some examples are shown in Fig. 3 for A = 1. Note that the most probable value of r for breakdown is approximately equal to r_1, and that the parameter α determines the sharpness of the distribution function.

Next, let us see how the distribution function N(r) changes as a function of area (frequency). This is shown in Fig. 4 for $\alpha = 3$ and $r_1 = 0.6$. To be specific, we have also taken H_{b1} to be 1500 G and A = 1 to represent the area of a cavity at 9 GHz. We assume, in scaling from one frequency to another, that all cavity dimensions are scaled in direct proportion to the wavelength; hence $f \sim A^{-1/2}$. It is seen that the most probable breakdown field shifts to lower frequencies with increasing cavity area, as we would expect. In Fig. 5 the most probable breakdown field is plotted as a function of frequency for several values of α and r_1, again assuming A = 1 at 9 GHz. It is easy to show that for low frequencies ($A \gg 1$) the most probable breakdown field appraoches a frequency dependence given by $f^{2/\alpha}$.

As a final example, let us suppose that the distribution function for A = 1, r = 0.6, and $\alpha = 3$ properly characterizes a good processing technique for TM mode cavities at 9 GHz. The peak is about right (910 G). Also, 10% of these cavities will have breakdown fields greater than 1000 G, and 10% will have breakdown fields less than 620 G. This is a reasonable sharpness for a good processing method. At lower frequencies, the most probable breakdown field then varies as shown in Table IV. Also

TABLE IV

VARIATION OF BREAKDOWN FIELD WITH FREQUENCY

$r_1 = 0.6, \quad \alpha = 3$

Frequency	Most Probable Breakdown Field	$H_b(10\%)$
9.0 GHz	910 G	1000 G
2.85	610	720
1.3	400	500
$1.3/\sqrt{21} = 0.28$*	180	250
$2.85/\sqrt{7} = 1.1$**	375	475

*Effective frequency for the HEPL pre-accelerator.

**Effective frequency for the HEPL 7-cell S-band structure.

listed is $H_b(10\%)$; 10% of the cavities should have greater breakdown fields than this field. The fourth entry in the table corresponds to a structure at 1.3 GHz with an area equivalent to 21 TM mode cavities, roughly representing the area of the HEPL pre-accelerator section with 21 excited cells. The last entry is for a structure at 2.85 GHz with 7 excited cells. The numbers in the table are in reasonable agreement with experimentally observed breakdown fields.[12]

Does the preceding analysis have any connection with the real world? The situation is much like that in thermodynamics; not much is know about the system (cavity surface) on a detailed level, but certain average tendencies are both predictable and unavoidable. Also, the preceding analysis does not rule out the possibility of an inherent frequency dependence for the breakdown field. The breakdown field H_{b1} for a homogeneous surface may vary due to trapped flux,[24] phonon generation[25], etc. However, the statistical effect discussed here may mask such an inherent frequency dependence, and must in any case be taken into consideration in drawing conclusions from the experimental observations.

Acknowledgements

The exacting experimental techniques required for the success of the gas exposure tests listed in Table III were developed by E. W. Hoyt. The fabrication, processing, and measurement of the X-band cavities used in these tests was carried out with the participation of H. A. Hogg, H. Deruyter, Z. D. Farkas, H. Martin and R. Silvers.

References

1. R. Benaroya et al., Appl. Phys. Lett. 21, 235 (1972).
2. H. Hahn, private communication.
3. M. Strongin et al., "Effect of Surface Conditions on Some Superconducting Properties of Niobium," 1972 Applied Superconductivity Conference, Annapolis, Md. Proceedings to be published.
4. H. J. Halama, Proceedings of the 8th International Conference on High Energy Accelerators, CERN, 1971 (CERN Scientific Information Service, Geneva, 1971), p. 242.
5. G. J. Dick and K. W. Shepard, "Phase Stabilization of Superconducting Helical Accelerating Structures," 1972 Applied Superconductivity Conference, Annapolis, Md. Proceedings to be published.
6. J. S. Allen et al., Particle Accelerators 1, 239 (1970).
7. A. O. Hanson, IEEE Trans. Nucl. Sci. NS-18, No. 3, 149 (1971).
8. C. M. Jones et al., Particle Accelerators 3, 103 (1972).
9. M. S. McAshan, H. A. Schwettman, L. Suelzle and J. P. Turneaure, "Development of the Superconducting Accelerator," HEPL Report No. 665, High Energy Physics Laboratory, Stanford University (January 1972).
10. R. E. Rand, "Multiple Recirculation of the SCA Beam," HEPL TN-72-2, High Energy Physics Laboratory, Stanford University (June 1972).
11. L. R. Suelzle and E. E. Chambers, "Beam Performance of the Superconducting Injector for the Stanford Superconducting Linear Electron Accelerator." Paper presented at this conference.
12. C. Lyneis, M. McAshan and V. Nguyen, "Recent Measurements of S-Band and L-Band Cavities at Stanford." Paper presented at this conference.
13. I. Ben-Zvi, J. G. Castle, Jr., and Peter H. Ceperley, IEEE Trans. Nucl. Sci. NS-19, No. 2, 226 (1972).
14. Peter H. Ceperley, IEEE Trans. Nucl. Sci. NS-19, No. 2, 217 (1972).
15. A. Brandelik et al., "First Operation of a Superconducting Proton Accelerator." Paper presented at this conference.
16. J. E. Vetter, B. Piosczyk, and J. L. Fricke, "A Summary of RF Measurements on Superconducting Helically Loaded Resonators." Paper presented at this conference.
17. W. Bauer et al., "Investigation of Niobium Deflecting Cavity Models for Use in a Superconducting RF Particle Separator," 1972 Applied Superconducting Conference, Annapolis, Md. Proceedings to be published.
18. A. Carne et al., Proceedings of the 8th International Conference on High Energy Accelerators, CERN, 1971 (CERN Scientific Information Service, Geneva, 1971), p. 249.
19. A. Brandelik et al., "RF Control and Tuning of Superconducting Helically Loaded Cavities," Paper presented at this conference.
20. G. Bathow, E. Freytag and H. O. Wüster, Das Mesotron-ein Elektronen Beschleuniger für hohe Endenergien. DESY 68/58 (December 1968). Translated in SLAC-TRANS-89, Stanford Linear Accelerator Center.
21. J. P. Turneaure, "The Status of Superconductivity for RF Applications," 1972 Applied Superconductivity Conference, Annapolis, Md. Proceedings to be published.
22. H. Diepers and H. Martens, Phys. Lett. 38A, 337 (1972).
23. I. S. Sidorenko and E. I. Revutskii, Sov. Phys. - Tech. Phys. 10, 583 (1965).
24. M. Rabinowitz, Appl. Phys. Lett. 19, 73 (1971).
25. C. Passow, Phys. Rev. Lett. 28, 427 (1972).
26. J. Halbritter, "RF Breakdown in Superconducting Cavities," 1972 Applied Superconductivity Conference, Annapolis, Md. Proceedings to be published.
27. K. Mittag, H. D. Schwarz, and H. A. Schwettman, "Beam Breakup Measurements in the Superconducting Electron Accelerator." Paper presented at this conference.
28. R. Benaroya et al., "Progress in Development of Superconducting Cavity for Heavy Ion Acceleration." Paper presented at this conference.
29. S. R. Stein and J. P. Turneaure, "Superconducting Cavity Stabilized Oscillators of 10^{-14} Stability." To be published in the proceedings of the 13th International Conference on Low Temperature Physics, Boulder, Colorado, August 1972.
30. T. Nishikawa, private communication.
31. N. G. Anishchenko et al., Proceedings of the 7th International Conference on High Energy Accelerators, Yerevan, USSR, August 1969, Vol. II, p. 638.
32. E. V. Khristenko et al., Sov. Phys. - Tech. Phys. 12, 1355 (1968).

Footnotes

†A recent survey of J. P. Turneaure, [21] covering the broader topic of the status of superconductivity for rf applications, contains much that is relevant to the topic discussed here. It is hoped that the material presented in this paper will complement Turneaure's summary.

††A more complete account of the gas exposures, with details of the exposure technique and additional test results, will be published at a later date.

†††The nitride layer is formed by heating the niobium to ~ 1400°K for several minutes in 1 atmosphere of nitrogen.

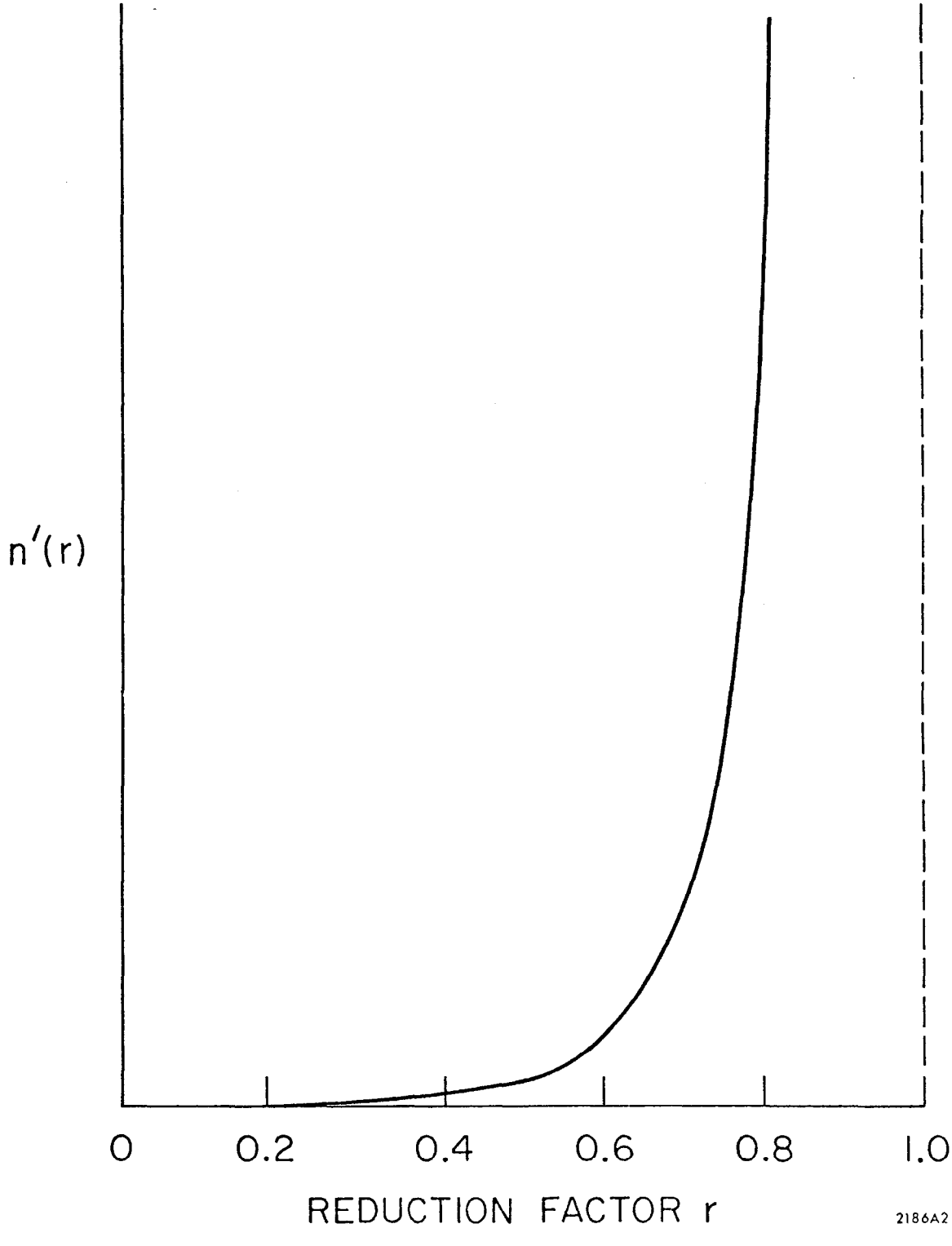

1. Typical variation for the relative number of defects as a function of the breakdown field reduction factor. The function shown is dn(r)/dr, where n(r) is given by Eq. (2) with α=2.

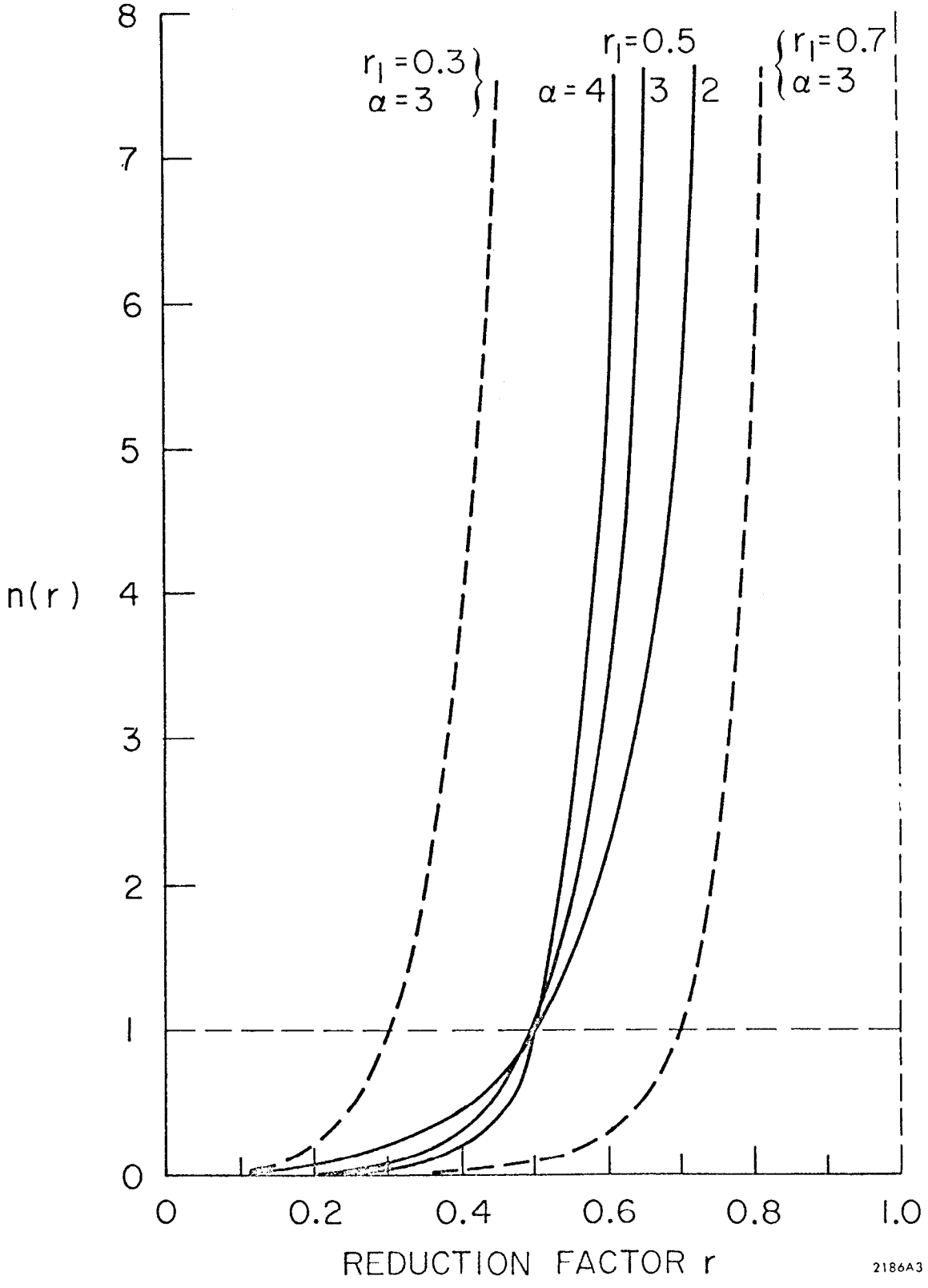

2. The function n(r), as given by Eq. (2), for several values of r and α.

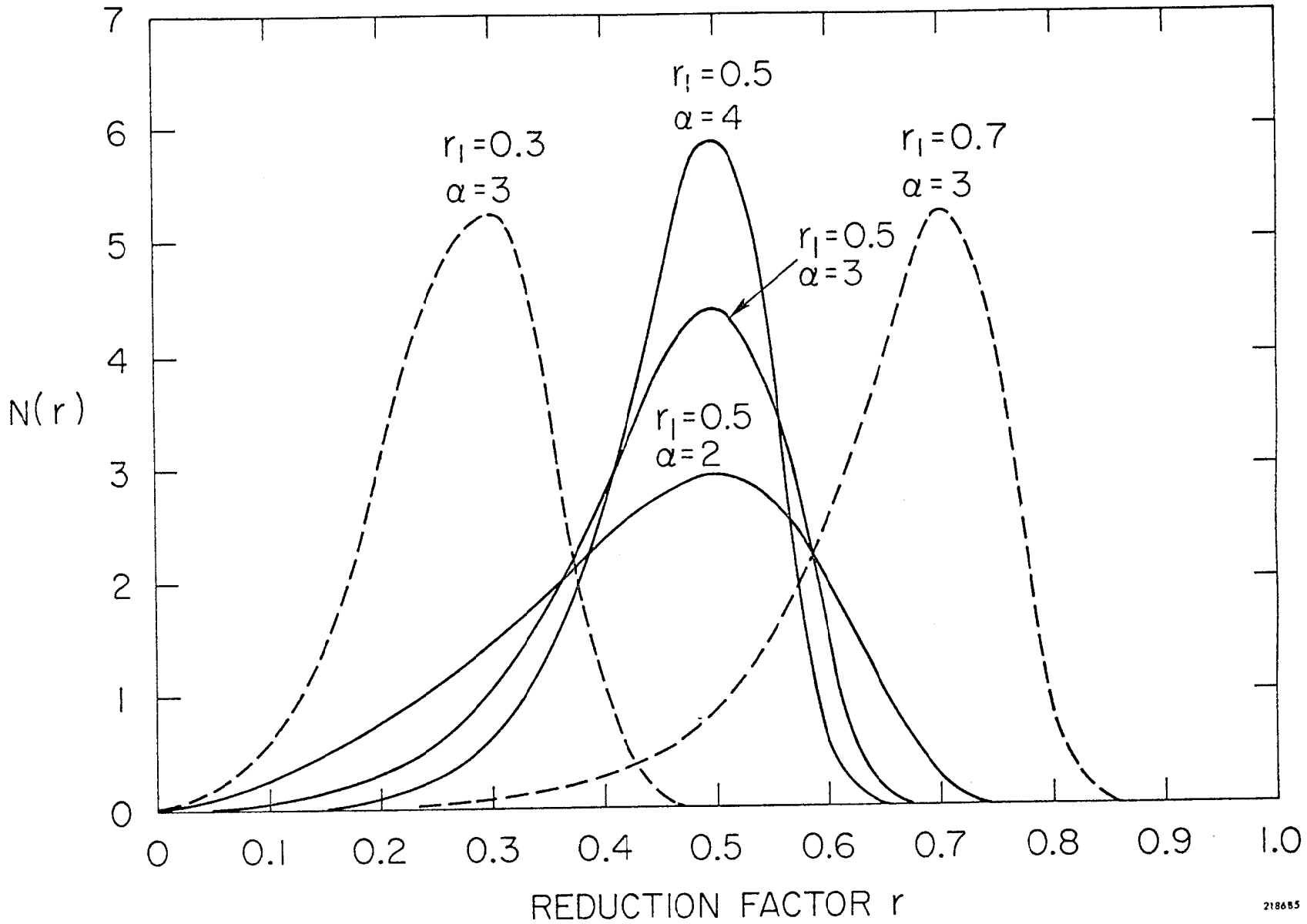

3. The function N(r), giving the probability of breakdown as a function of rf magnetic field level rH_{b1}, for the corresponding functions n(r) shown in Fig. 2.

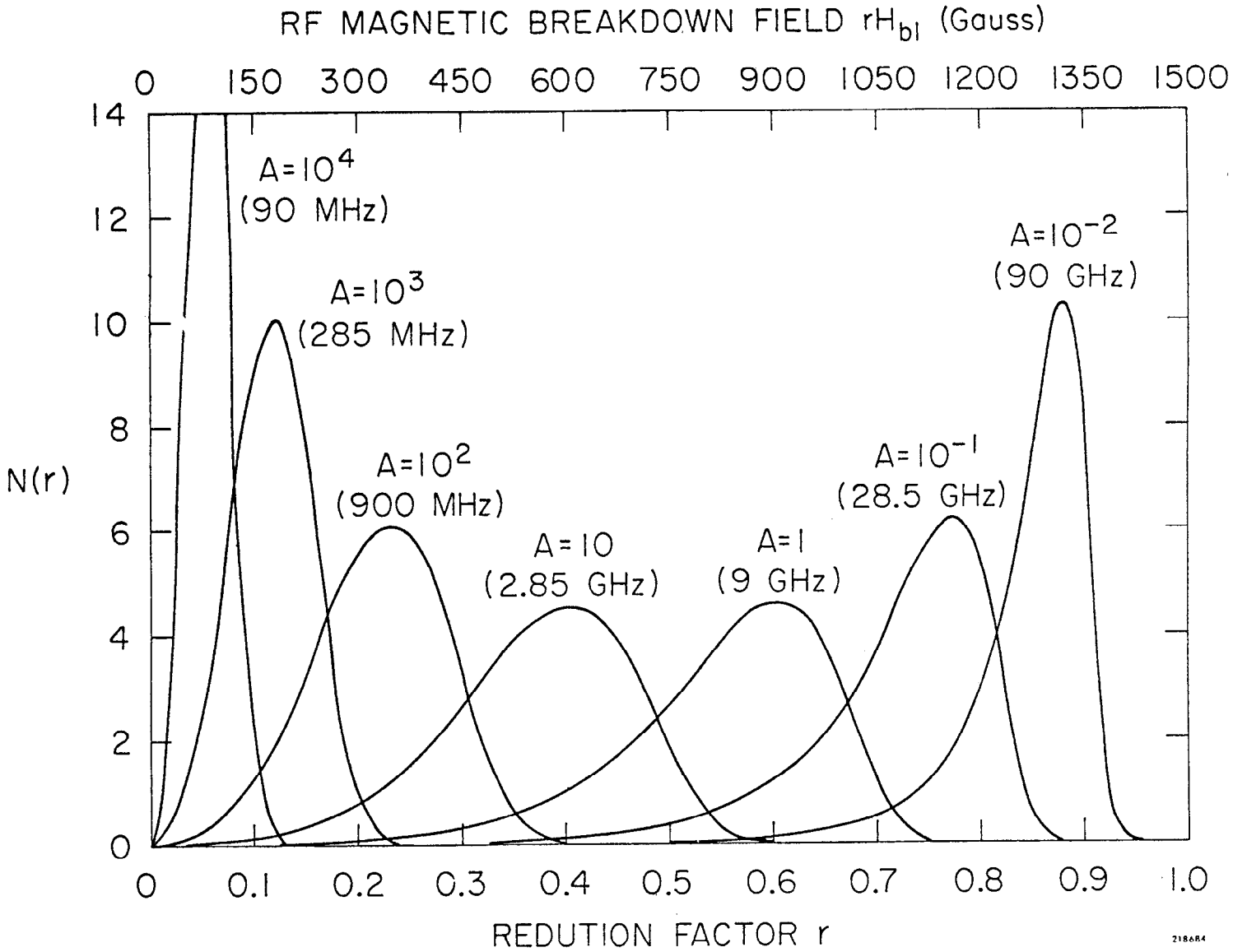

4. Plots of the breakdown field distribution function N(r) as a function of rf magnetic field level for various values of the cavity area parameter A. Here r_1=0.6, α=3, and H_{b1}=1500 G.

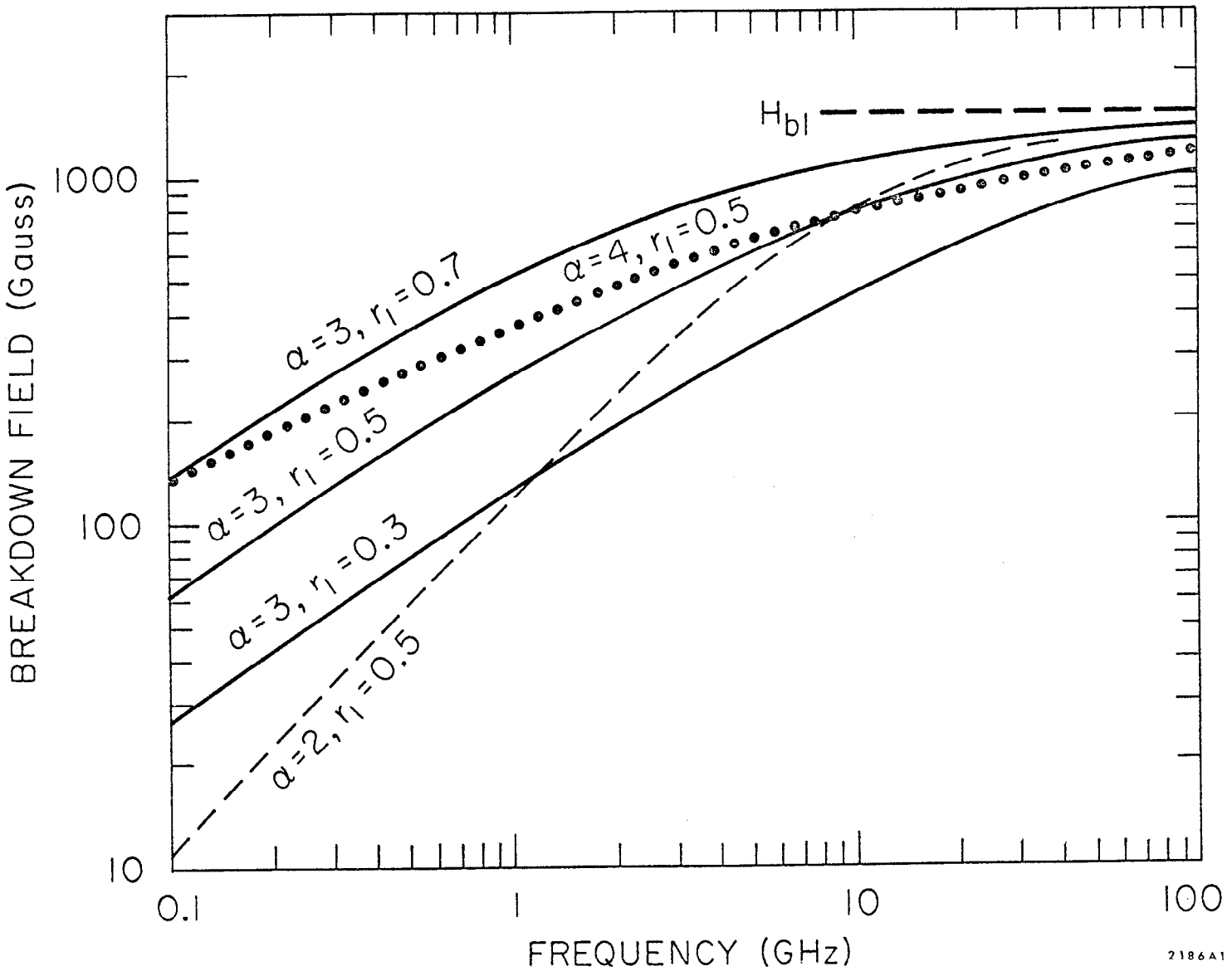

5. The most probable breakdown field as a function of frequency for various values of the parameters α and r_1, with $H_{b1} = 1500$ G.